Edwin I. Hatch Nuclear Plant – Unit 2
Submittal of Additional Information to Support Proposed Exemption to 10 CFR 50.46 and 10 CFR 50 Appendix K to Allow Ziron Fuel Cladding

Enclosure 6

GNF-0000-0088-6043NP,
"Properties of GNF-Ziron" July 2008
(Nonproprietary)

Global Nuclear Fuel

A Joint Venture of GE, Toshiba, & Hitachi

GNF-0000-0088-6043NP
Class I
July 2008

Non-Proprietary Information

Properties of GNF-Ziron

INFORMATION NOTICE

This document is a non-proprietary version of GNF-0000-0088-6043P which has the proprietary information removed. The information removed is shown as blank between double brackets [[ ]].

IMPORTANT NOTICE REGARDING CONTENTS OF THIS REPORT PLEASE READ CAREFULLY

The information contained in this document is furnished for the purpose of providing information supporting the installation of fuel assemblies containing lead test quantities of GNF-Ziron cladding. The only undertakings of Global Nuclear Fuel-Americas, LLC (GNF) with respect to information in this document are contained in contracts between GNF and its customers, and nothing contained in this document shall be construed as changing those contracts. The use of this information by anyone other than those participating entities and for any purposes other than those for which it is intended is not authorized; and with respect to any unauthorized use, GNF makes no representation or warranty, and assumes no liability as to the completeness, accuracy, or usefulness of the information contained in this document.

Properties of GNF-Ziron

A modified Zircaloy, described here as GNF-Ziron, has been under development and testing by GE/GNF over the last two decades. The composition of GNF-Ziron is modified from that of Zircaloy-2. The primary modification is in the iron content, which is adjusted to be above the range specified in the ASTM B350 industry standard. GNF-Ziron has a Fe specification of [[ ]] compared with a 0.20 wt% upper limit for Zircaloy-2; [[ ]]. The earlier development work had led to a Lead Use Assembly (LUA) program at a European reactor starting in 1999. In that 1999 LUA program, GNF-Ziron was used as the cladding, spacer and water rod materials. The LUA bundles have reached bundle average exposure of about [[ ]] GWd/MTU in October of 2005. Based on positive indications from poolside inspections and recent new data on the GNF-Ziron alloy, GNF is interested in pursuing the alloy for reload applications, for which approval from the NRC will be required. It is expected that additional hotcell results and test data will be needed prior to the submittal to the NRC for approval of GNF-Ziron as a fuel assembly alloy. In the interim, GNF is actively pursuing a wider application of GNF-Ziron through additional Lead Test Assembly (LTA) programs with several utilities. This document is being prepared to support the LTA programs.

In support of the 1999 LUA program, available information was compiled in 1999 for review by the appropriate regulator. The data reviewed remain unchanged since 1999. The present review updates the 1999 report with additional recent data on GNF-Ziron.

Considering the small change of the overall alloying chemistry between Zircaloy-2 and GNF-Ziron (typically [[ ]] Fe for Zircaloy-2 vs. [[ ]] Fe for GNF-Ziron) and that both alloys are processed similarly to yield a recrystallize-annealed microsctructure, a number of properties are considered not to be significantly affected and there has been no new data generated specific to GNF-Ziron. These properties are listed in Table 1.

Other properties were considered to be potentially affected by the change in alloy chemistry and therefore may need supporting data. The supporting data available in 1999 were generated from coupons or test pieces irradiated at the Advanced Test Reactor (ATR) and [[ ]] reactor in the US, the Halden test reactor in Norway and [[ ]]. The available [[ ]] data were limited to mostly 2 cycles of irradiation in the 1999 report. Since 1999, new data from post-irradiation examination and testing following 6 cycles exposures at [[ ]] reactor and poolside examination results from the 1999 LUA program have been obtained. These properties as discussed below:

Stress-Strain Relations for Zirconium Alloys

Tensile properties of GNF-Ziron were determined from specimens irradiated in the ATR in the US and [[ ]]. The ATR irradiations were carried out at a nominal irradiation temperature of 300°C ±25°C. The Zircaloy-2 and GNF-Ziron specimens were discharged at fluences of between [[ ]] x 10^{21} n/cm^2. The mechanical properties obtained from these tests conducted at 300°C are summarized in Table 2. The results show that the strength properties of GNF-Ziron are higher. However, the ductility after irradiation in tensile tests, as seen by the values of total elongation and reduction in area, shown in Table 2 is still quite high.

Tensile properties at 23°C, 288°C and 343°C (300K, 561K and 616K) were conducted following 1, 2, 4 and 6 cycles of irradiation in the [[ ]] reactor. The highest fast neutron fluence reached was about 15 x 10^{21} n/cm^2. The variation of ultimate tensile strength (UTS) and total elongation (TE) with fluence at the three test temperatures for Zircaloy-2 and GNF-Ziron are shown in Figures 1 and 2 together with those of a High FeNi Zr-alloy*. The results shown in Figures 1 and 2 confirm the results from the ATR specimens, Table 2, and show that GNF-Ziron possesses higher strength without any adverse effect on ductility. The results from [[ ]] specimens show the expected general trend to saturate beyond a fast neutron fluence of about 3.5 x 10^{21}n/cm^2, typical of tensile properties of zirconium-based alloys. A deviation from the saturating trend can be noted for the total elongation of Zircaloy-2 following 6 cycles of irradiation. The 6 cycles Zircaloy-2 specimens exhibited low elongations at all three test temperatures. The difference in the stress-strain behaviors of GNF-Ziron and Zircaloy-2 after 6 cycles of irradiation is further illustrated in Figure 3. The reduction in ductility for Zircaloy-2 is due to the high concentrations of absorbed hydrogen in the 6-cycles specimens. (Hydrogen absorption characteristics are discussed in a later section.)

The available data support the use of the current Zircaloy-2 stress-strain relations (which does not include effects due to high hydrogen concentrations) for design analyses of fuel with GNF-Ziron cladding, as in general the GNF-Ziron possesses higher strength without any adverse effect on ductility.

Meyer Hardness of Zirconium Alloys

The hardness data are used in design analysis to characterize the behavior of the interface between the fuel and a non-barrier cladding. Although no Meyer hardness data were generated, micro-Vickers hardness data were obtained from GNF-Ziron following irradiation in [[ ]] reactor and tested at 300K using a 300g load and a 15s loading time. The micro-Vickers hardness of GNF-Ziron as a function of fast neutron fluence is shown in Figure 4 together with those of Zircaloy-2. GNF-Ziron has a slightly higher initial hardness than Zircaloy-2 in the unirradiated state. Hardness after irradiation is also slightly higher, however, the tendency of the hardness to saturate with fluence is similar for all alloys.

* In this report, graphs have been reproduced from other reports which included this material; this material is not discussed in the report because it is not germane to the discussion on GNF-Ziron.

In the absence of Meyer hardness data specific to GNF-Ziron, the Meyer hardness could be estimated from the yield strength of the alloy. The tensile properties of GNF-Ziron discussed in the previous section show that the yield strength of the alloy is slightly higher than Zircaloy-2. The estimated Meyer hardness based on the tensile properties of samples irradiated at ATR is shown in the last column of Table 2. Since tensile flow properties generally saturate above about 3.5 x 10^{21}n/cm^2, the yield strength and hence estimated Meyer hardness values in Table 2 could be taken to represent the cladding behavior at higher fluences. The potential change in Meyer hardness level is [[ ]] to the thermal-mechanical behavior of the fuel.

Zirconium Alloys Cyclic Stress - Strain Curve

For the temperature range of interest to BWR applications (260 - 320°C) the cyclic stress-strain curves for Zircaloys and zirconium have been related to their respective monotonic stress-strain curves to account for hardening/softening due to cycling. As discussed under *Stress-Strain Relations for Zirconium Alloys*, a high concentration of absorbed hydrogen in Zircaloy-2 can result in low tensile ductility following high exposures. However, GNF-Ziron at a similar exposure (6 cycles and 15 x 10^{21} n/cm^2) exhibited stress-strain behavior similar to Zircaloy-2 with low hydrogen concentrations. In view of the fact that these applications of the monotonic stress-strain curves (without taking into account hydrogen effects on Zircaloy-2 at high exposures) have been used successfully for zirconium and Zircaloy-2, it is expected that the same applications can be used for the slightly modified compositions of GNF-Ziron.

Zircaloy Strain to Failure

The macroscopic strains to failure for the GNF-Ziron are expected to be [[ ]] Zircaloy-2 with low hydrogen concentrations, since the post-irradiation tensile stress-strain curves [[ ]] and the ductility is [[ ]], as represented by the total elongation and reduction in area. The correlation for the microscopic or local strain to failure for Zircaloy-2 is based on experimental data extrapolated using finite element analysis. Since the ductility of GNF-Ziron from the ATR and [[ ]] irradiations is [[ ]] the ductility of Zircaloy-2 with low hydrogen concentrations, the microscopic or local strain to failure for GNF-Ziron could be expected to be [[ ]] as for Zircaloy-2. [[ ]]

Creep

The creep strain behavior of GNF-Ziron, High FeNi Zr-alloy and Zircaloy-2 up to 6 cycles of irradiation in [[ ]] reactor is shown in Figure 5. The creep strength of these materials appears to be higher than that of Zircaloy-2. While the creep strength of GNF-Ziron is higher, i.e. a lower creep rate for a given stress, the overall creep behavior is [[ ]] observed from a number of different experiments. The creep of GNF-Ziron will be modeled using [[ ]].

The extent of improvement in creep strength is [[
]] a new correlation.

Zirconium Alloys Stress Rupture

No new data has been obtained since 1999. The stress rupture correlation for Zircaloy will continue to be used for GNF-Ziron.

Zirconium Alloys Fatigue Design Curve

Fatigue testing at different strain amplitudes has been conducted on Zircaloy-2 and GNF-Ziron following irradiation for up to 6 cycles in [[ ]] reactor. The results are presented in Figure 6 together with the reference fatigue curve based on O'Donnell and Langer's 1964 work. The cycles to failure for 0.55% strain amplitude are shown in Figure 7. Figures 6 and 7 show that there is no significant difference in fatigue behavior between Zircaloy-2 and GNF-Ziron. In Figure 6, it is seen that in all cases the number of cycles to failure for a given total strain amplitude falls above the reference correlation, [[ ]]

Irradiation Growth of Zirconium Alloys

In the 1999 report, relevant growth data obtained from irradiations at ATR to ~6.0 x 10^{21} n/cm^2 indicated similar irradiation growth behavior for Zircaloy-2 and other alloys including GNF-Ziron. An irradiation growth program is currently underway aimed at providing growth data up to [[ ]] x 10^{21} n/cm^2, and the results have not yet been made available. In the absence of new irradiation growth data for GNF-Ziron, indirect data indicating [[ ]] irradiation growth characteristics for GNF-Ziron compared with Zircaloy-2 have been obtained from poolside inspections of the 1999 LUA program. Figure 8 shows the 5 and 6 cycles water rod growth data for GNF-Ziron compared with Zircaloy-2 in the LUA program. The Zircaloy-2 data also included measurements made from other poolside inspections at similar exposures. The water rod growth data show that GNF-Ziron growth data are [[ ]] of the Zircaloy-2 experience, irrespective of consideration based on irradiation time or bundle average exposure. Figure 9 shows the 5 cycles spacer width data for GNF-Ziron compared with Zircaloy-2 data obtained from poolside inspections at other plants. The spacer width data show that GNF-Ziron spacers appear to [[ ]] Zircaloy-2 spacers of similar bundle average exposure; however,
[[ ]]. The water rod and spacer growth data do not provide a direct comparison of irradiation growth behavior of the different alloys, since other factors such as absorbed hydrogen could affect the dimensional measurements. Nonetheless, the water rod growth and spacer width data from the 1999 LUA program is consistent with GNF-Ziron having [[ ]] irradiation growth behavior as Zircaloy-2. Based on available information, the growth behavior of GNF-Ziron will be modeled using [[ ]].

Corrosion of Zirconium Alloys in BWR Service

Corrosion data (oxide thickness and absorbed hydrogen) for GNF-Ziron irradiated at [[ ]] were reviewed previously, which also included post-irradiation corrosion test results. Since 1999, corrosion and hydriding data following high exposures in [[ ]] reactor have become available. Figures 10a and 10b show the corrosion behavior of GNF-Ziron and Zircaloy-2 following 1, 2, 4 and 6 cycles of irradiation. The surface appearances are shown in Figure 11. Up to 4 cycles (~1700 days) of irradiation, GNF-Ziron and Zircaloy-2 showed similarly low levels of corrosion, Figures 10a and 11. A large enhancement in corrosion for some samples resulting in a large scatter in the weight gain data was observed after 6 cycles (~2500 days). The increased corrosion after 6 cycles can be related to the more extensive presence of patchy oxide as shown in Figure 11. The weight gain data and visual appearances did not show any significant difference between Zircaloy-2 and GNF-Ziron.

The hydrogen pickup behavior of GNF-Ziron and Zircaloy-2 is shown in Figure 12. Similar to corrosion weight gain, hydrogen uptake for GNF-Ziron and Zircaloy-2 was generally low up to 4 cycles of irradiation, and a clear enhancement in hydrogen pickup occurred between 4 and 6 cycles of irradiation. Hydrogen pickup data from [[ ]] reactor for GNF-Ziron after 6 cycles is only available for samples irradiated in high flux locations. Figure 12 shows that GNF-Ziron exhibited [[ ]] in hydrogen pickup, especially compared with Zircaloy-2. The difference in hydrogen contents between Zircaloy-2 and GNF-Ziron, particularly after 6 cycles, is also evident by the amounts of zirconium hydride precipitates, as shown in Figure 13.

The difference in hydrogen pickup characteristics between GNF-Ziron and Zircaloy-2 is more evident when the hydrogen absorbed due to corrosion is expressed as a fraction or percentage of the total amount of hydrogen generated by the corrosion reaction. The percentage hydrogen pickup data is shown in Figure 14. Figure 14 shows that GNF-Ziron has [[ ]] of absorbed hydrogen, even [[ ]]. A low hydrogen pickup from [[ ]] irradiation program is consistent with prior results from ATR and [[ ]].

The corrosion and hydriding tests at [[ ]] and ATR were conducted on sheet or un-fueled cladding coupons. Fueled cladding was tested in the 1999 LUA program. In the LUA program, selected assemblies had cladding manufactured from GNF-Ziron and some of the GNF-Ziron assemblies had the water rod and spacers manufactured from GNF-Ziron. Selected GNF-Ziron bundles were inspected at different stages of exposure and the companion Zircaloy-2 bundles were [[ ]] GWd/MTU. Poolside eddy current liftoff inspection results for GNF-Ziron are shown in Figure 15. Figure 15 also shows GNF's liftoff experience base up to [[ ]] GWd/MTU.
[[

]] Figure 15 shows that the corrosion performance of GNF-Ziron cladding is [[ ]] GNF's experience base that was developed on Zircaloy-2 cladding. In the high exposure range (above [[ ]]GWd/MTU) the GNF-Ziron data [[

]] an extrapolation of the experience base, as confirmed by [[ ]] liftoff for GNF-Ziron and Zircaloy-2 measured at [[ ]] GWd/MTU. [[ ]] in corrosion behavior between GNF-Ziron and Zircaloy-2 as indicated by the liftoff data, figure 15, is supported by visual examinations of the claddings. Figures 16 and 17 show, respectively, representative appearances of the GNF-Ziron and Zircaloy-2 claddings at [[ ]] GWd/MTU bundle average exposure. The 1999 LUA program also included many segmented rods that covered a broader range of cladding manufacturing conditions, such as solid vs. hollow billet quench and Tube-Shell Heat Treat (TSHT) vs. In-Process Heat Treat (IPHT). The eddy current liftoff data from the fueled region of the segmented rods are shown in Figure 18. Similar to the results from full-length rods, Figure 15, [[ ]] between GNF-Ziron and Zircaloy-2 or between different cladding heat treatments was [[ ]].

In summary, available corrosion information indicates [[ ]] corrosion performance between GNF-Ziron and Zircaloy-2. A significant difference in the hydrogen absorption characteristics has been noted, with the GNF-Ziron exhibiting significantly lower hydrogen pickup compared with Zircaloy-2. [[ ]].

Zirconium Alloy Clad Rupture

A design correlation to determine the perforation temperature for standard and barrier Zircaloy fuel clad under internal pressure and rapid heating conditions is currently available for Zircaloy-2. Such a correlation has been presented as a function of engineering hoop stress for heating rates [[ ]]C/sec in the temperature range [[ ]]. Data have been generated for the GNF-Ziron to verify the applicability of this correlation. Tests were conducted with target burst pressures between [[ ]] at a heating rate of [[ ]]. The burst test results for GNF-Ziron are shown in Figure 19 and the visual appearance of some of the test pieces are shown in Figure 20. The burst test results show that the hoop strain at perforation is larger than [[ ]] and that the cladding temperature at perforation tends to [[ ]]. In Figure 21, the data for GNF-Ziron is compared with data for Zircaloy-2. The comparison shows that the hoop stress for perforation of GNF-Ziron cladding [[ ]].

Simulated LOCA and quench tests

Oxidation kinetics under simulated LOCA conditions and quench ductility under constraining loading have been obtained for GNF-Ziron. The high temperature oxidation tests were conducted at [[ ]]. The weight gain data are shown in Figure 22 and the measured reaction constants compared with literature data are shown in Figure 23. The results indicate that at both test temperatures the oxidation kinetics of GNF-Ziron are lower than those predicted by the Baker-Just or Cathcart-Pawel relationships.

Tests on GNF-Ziron under a restraining load were conducted at [[
]], with cladding oxidized to [[ ]] Effective Cladding Reacted (ECR) (based on Baker-Just) at [[ ]] and to [[
]]C. The results showed that cladding oxidized to [[ ]] ECR and less did not fail and that only the cladding oxidized to [[ ]] ECR failed.

Table 1 Material Properties Expected to be Nearly Identical to Zircaloy-2

[[

]]

Table 2 Material Properties of samples irradiated at ATR tested at 300°C

[[

]]

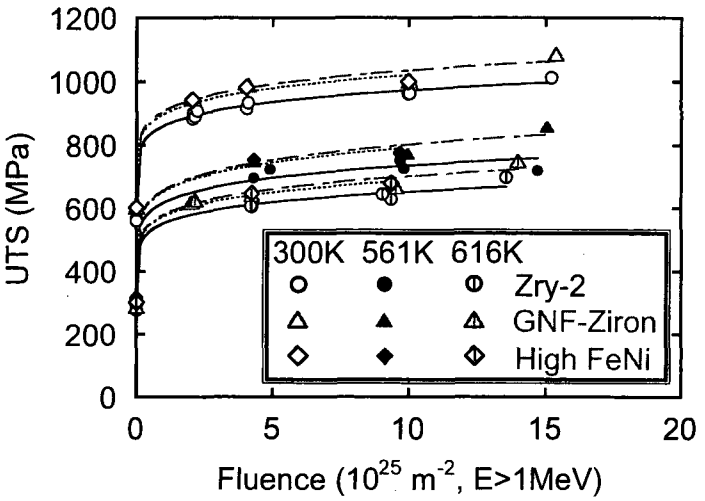

Figure 1 Variation of UTS with fast neutron fluence at three test temperatures for Zircaloy-2, GNF-Ziron and a High FeNi Zr-alloy.

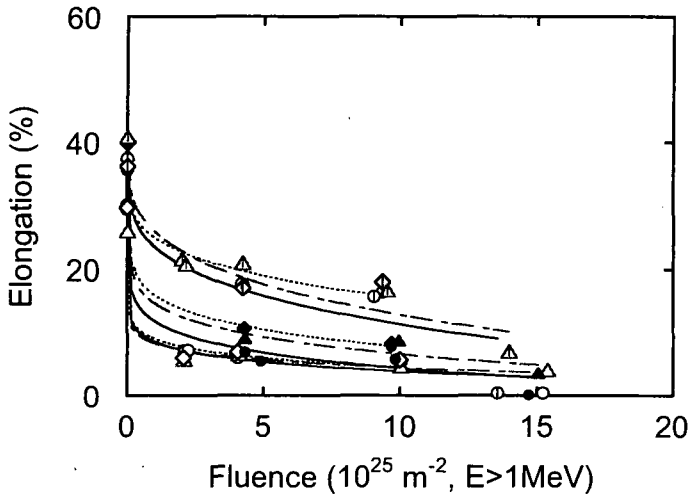

Figure 2 Variation of total elongation with fast neutron fluence at three test temperatures for Zircaloy-2, GNF-Ziron and a High FeNi Zr-alloy. (See Figure 1 for legends)

[[

]]

Figure 3 Comparison of 300K stress-strain curves for Zircaloy-2 and GNF-Ziron following 6 cycles of irradiation in [[ ]] reactor.

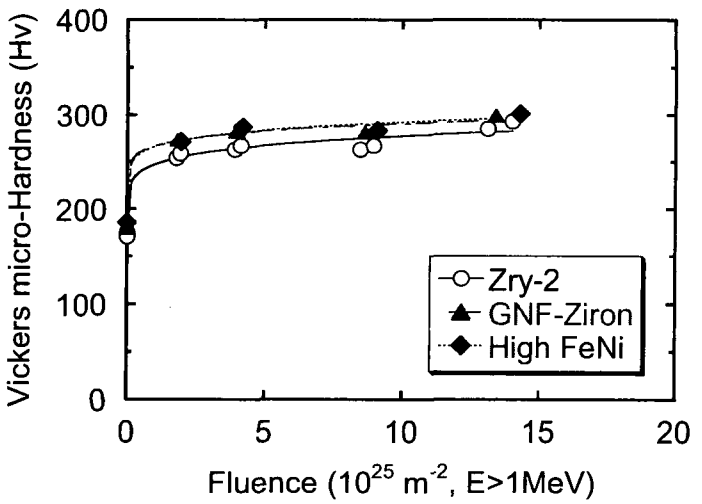

Figure 4 Micro-Vickers hardness for Zircaloy-2, GNF-Ziron and a High FeNi Zr-alloy as a function of fast neutron fluence following irradiation in [[ ]] reactor and tested at 300K.

a)

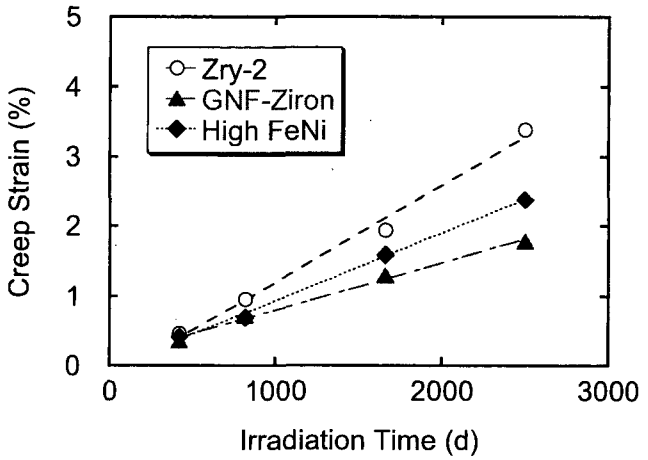

b)

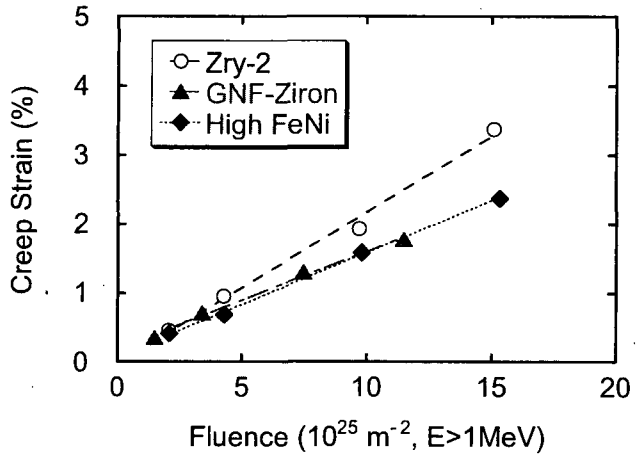

Figure 5 Creep behavior of Zircaloy-2, GNF-Ziron and a High FeNi Zr-alloy as a function of a) irradiation time and b) fast neutron fluence in [[ ]] reactor under 150 MPa circumferential stress under irradiation.

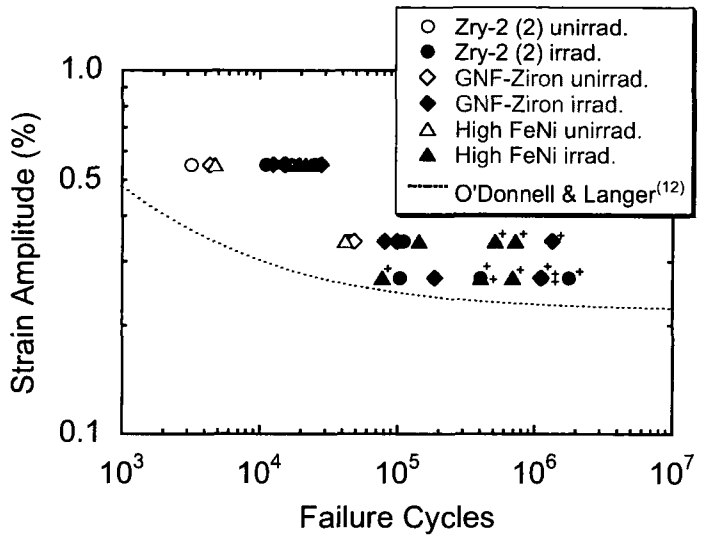

Figure 6 Fatigue behavior of unirradiated and irradiated Zircaloy-2, GNF-Ziron and a High FeNi Zr-alloy tested at 623K.

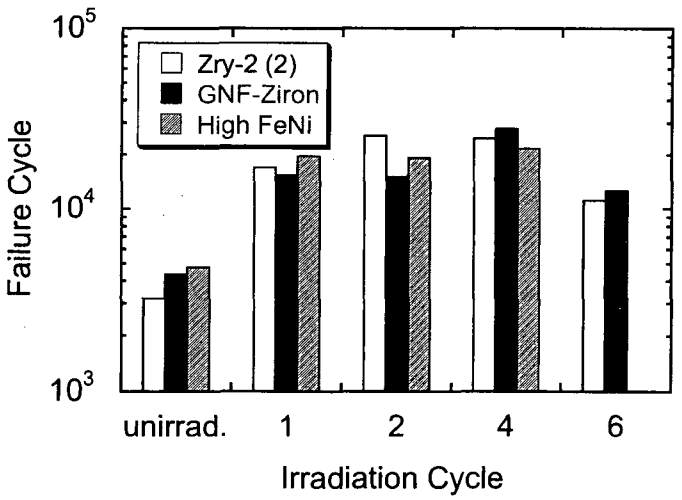

Figure 7 Fatigue cycles to failure for unirradiated and irradiated Zircaloy-2, GNF-Ziron and a High FeNi Zr-alloy tested at 623K under 0.55% strain amplitude.

a)
[[

b)

]]

Figure 8 Water rod growth of Zircaloy-2, GNF-Ziron and other alloys as a function of a) bundle average exposure and b) irradiation time from the 1999 LUA program. Data for Zircaloy-2 water rods from other inspections are included for comparison.

a)
[[

b)

]]
Figure 9 Spacer width measurements for Zircaloy-2, GNF-Ziron and other alloys as a function of a) bundle average exposure and b) irradiation time from the 1999 LUA program. Data for Zircaloy-2 spacers from other inspections are included for comparison.

a)

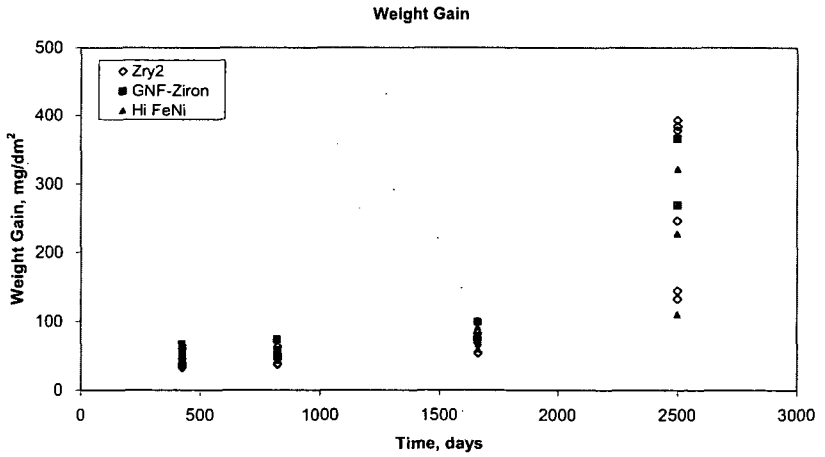

b)

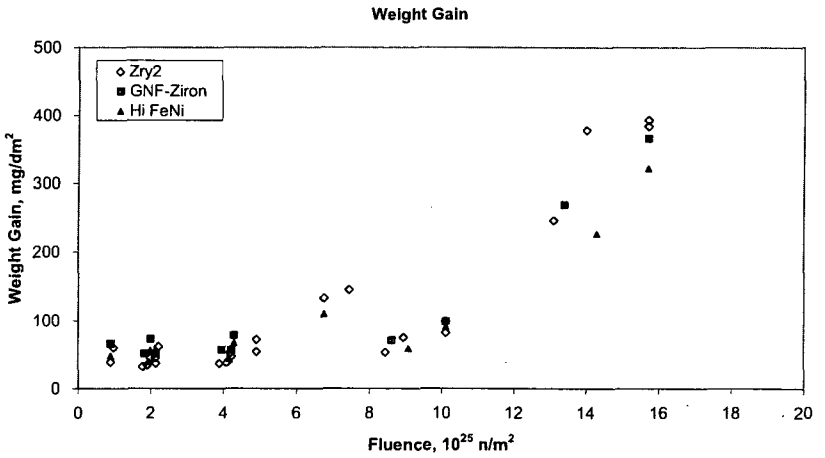

Figure 10 Corrosion weight gain data for Zircaloy-2, GNF-Ziron and High FeNi Zr-alloy following irradiation in [[ ]] reactor for 1, 2, 4 and 6 cycles as a function of irradiation time (a) and accumulated fast neutron fluence (b).

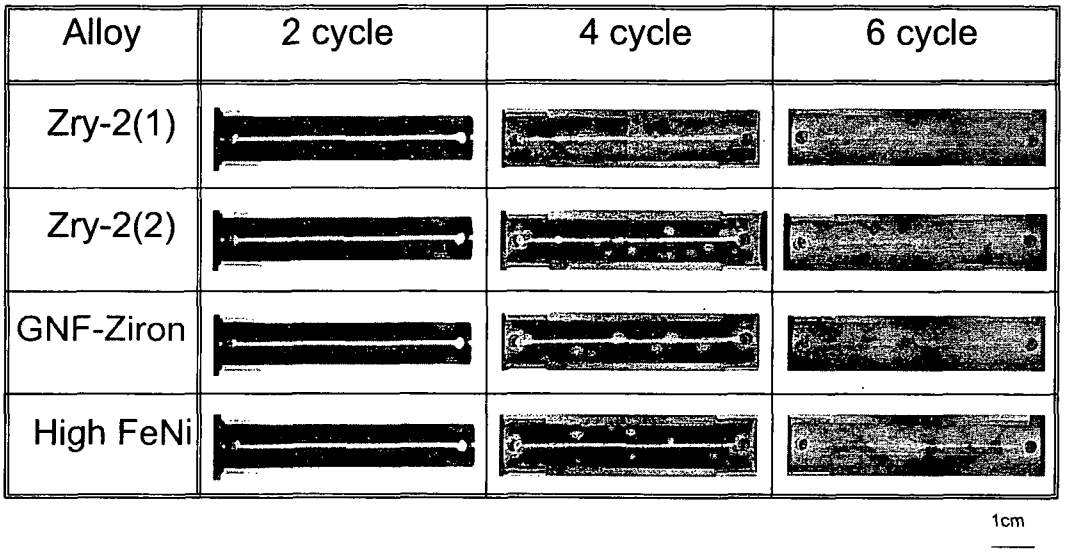

Figure 11 Visual appearance of corrosion test pieces of Zircaloy-2, GNF-Ziron and High FeNi Zr-alloy following irradiation in [[ ]] reactor for 2, 4 and 6 cycle.

[[

]]

Figure 12 Hydrogen content data for Zircaloy-2, GNF-Ziron and High FeNi Zr-alloy following irradiation in [[ ]] reactor for 1, 2, 4 and 6 cycles as a function of accumulated fast neutron fluence.

[[

]]

Figure 13 Metallographs showing zirconium hydride precipitates (gray) in Zircaloy-2, GNF-Ziron and High FeNi Zr-alloy after irradiation in [[ ]] reactor for 2, 4 and 6 cycles.

[[

]]

Figure 14 Hydrogen pickup percentage data for Zircaloy-2, GNF-Ziron and High FeNi Zr-alloy following irradiation in [[ ]] reactor for 1, 2, 4 and 6 cycles as a function of accumulated fast neutron fluence.

[[

]]

Figure 15 Eddy current liftoff results for GNF-Ziron cladding from the 1999 LUA program.

[[

]]
Figure 16 Representative appearances of the GNF-Ziron cladding at [[ ]] GWd/MTU bundle average exposure.

[[

]]
Figure 17 Representative appearances of the Zircaloy-2 cladding at [[ ]] GWd/MTU bundle average exposure.

[[

]]
Figure 18 Eddy current liftoff results from fueled region of segmented rods with GNF-Ziron, Zircaloy-2 and High FeNi Zr-alloy claddings after 4, 5 and 6 cycles of irradiation in the 1999 LUA program. The indicated exposures are approximate, since the data points have been juxtaposed for clarity.

[[

]]
Figure 19 High temperature burst test data for GNF-Ziron.

[[

]]

Figure 20 Visual appearance of some of the GNF-Ziron burst test pieces.

[[

]]

Figure 21 High temperature burst test data. GNF-Ziron data are shown by the red triangles.

[[

]]

Figure 22 GNF-Ziron oxidations kinetics at [[ ]].

[[

]]

Figure 23 GNF-Ziron (High Fe Zry) oxidations reaction constants compared with literature data.